SIDE JET FORMATION AND SPLIT FLAMES

John D. Carlton, Jean R. Hertzberg and Katharina Foerster
Center for Combustion and Environmental Research
University of Colorado, Boulder, Colorado 80309-0427, USA.

Mark A. Linne
Center for Combustion and Environmental Research, Division of Engineering
Colorado School of Mines, Golden, Colorado 80401, USA.

ABSTRACT

High-amplitude fuel jet forcing has been found to result in dramatic changes to a transitional nonpremixed methane flame shape: over a range of excitation frequencies the flame can be driven to split into a central jet and one or two side jets. The split is accompanied by a partial detachment of the flame from the nozzle exit, a shortening of the flame by a factor of two, and a change in flame color from yellow to blue. The forcing frequencies required to drive the flame to split correspond to the acoustic resonances of the combustor plenum. Under some conditions, the flame bifurcates between a split state and a typical transitional nonpremixed flame.

Flow visualization has revealed that the flame splits in response to side jet formation in the fuel jet. A nonreacting fuel jet was observed to split along both the major and minor axes under strong axial velocity perturbation. At less than one nozzle diameter downstream of the exit, side jets form along the major axis of the elliptic cross-section nozzle and continue to develop until approximately five diameters downstream. Pairs of streamwise vortex structures are observed in the side jets adjacent to the roller. Additional structure is seen in the side jets further from the roller, suggesting that fluid there had been ejected in streamwise structures from previous cycles.

We propose that side jets are the result of a reconnection event involving pairs of streamwise braid structures. The resulting loops then propagate perpendicular to the jet due to self induction. Self induction thus provides the mechanism for convection of fluid far from the jet. The evidence of streamwise vortex structures in the side jets and the position of braid structures relative to the rollers support this hypothesis.

INTRODUCTION

Recent fundamental investigations of transitional, forced axisymmetric diffusion flames have led to increased understanding of the role of shear layer dynamics in the transition to turbulence of these flames (Mahalingam et al., 1990; Katta and Roquemore, 1993). Experimental studies of the stabilization process of fully turbulent lifted jet flames (Schemer et al., 1994) have illustrated the importance of large scale shear layer structures and their three-dimensional evolution in time. These results have important consequences for the control of efficiency and pollutant formation in laminar and turbulent jet flames via passive and active shear layer control techniques. Here, 'passive technique' refers to manipulation of the system geometry to influence the three dimensional dynamics of vortex structures, and 'active' refers to any technique which adds energy (acoustic or kinetic) to the flow to influence the shear layer vortex dynamics. However, while entrainment and mixing in isothermal jets are easily controlled by such forcing techniques, jet diffusion flames are more difficult to control for several reasons: both hydrogen and hydrocarbon flames form on the outer edges of the shear layer region (Clemens and Paul, 1995), and the effects of heat release (with the exception of buoyancy) act to stabilize the flow. In fact, Hosangadi et al. (1990) state that the forcing of fuel jets offers little prospect for controlling a diffusion flame.

Nevertheless, high amplitude active forcing has been found to have a profound effect on a jet diffusion flame (Hertzberg, 1997; Carlton et al., 1998). Over a range of excitation frequencies the flame can be driven to split into a central jet and one or two side jets as shown in Figure 1. The split is accompanied by a partial detachment of the flame from the nozzle exit, a shortening of the flame by a factor of two, and a change from the common yellow color of soot

radiation to a predominantly clear blue flame. Yellow flame tips are sometimes observed. Flow visualization has shown that the flame splits in response to side jet formation in the fuel jet (Carlton et al., 1998). Under some conditions, the flame bifurcated in time between a split state and a classic transitional diffusion flame. The split flame may represent a useful approach to emission control using simple open-loop forcing. In addition, an understanding of how the flame can intermittently suppress and fail to suppress side jet formation could lead to greater control of flame/ flow instability interactions and hence expanded control of flame behavior. Further, the presence of bifurcation behavior suggests that a dynamical systems approach may be fruitful.

Similar behavior has been observed in two combustor geometries. Conditions for creating a split flame in a fully axisymmetric combustor are described in Hertzberg (1997). The present paper describes experimental results from a rectangular plenum with an elliptic nozzle configuration. The elliptic nozzle cross-section provides a well-defined azimuthal perturbation to the fuel jet, and it also helps stabilize the azimuthal position of the side jets. Laser sheet visualization of vertical and horizontal cross-sections is used to examine the development of side jets in reacting and nonreacting flow, and a mechanism leading to side jet formation is proposed. Conditions resulting in split flames for this combustor are also presented.

EXPERIMENTAL DESCRIPTION

The combustor schematic is shown in Fig 2. The combustor plenum is made up of two chambers connected by a 16.5 cm loudspeaker. The loudspeaker is driven by a sinusoidal signal between 500 and 600 Hz and 0 to 35 volts peak to peak, resulting fuel flow perturbations of up to 175%. The 2:1 aspect ratio elliptic cross sectioned (2.5 X 5.0 mm) methane jet issues from a flat plate; no co-flow is used. The bulk velocity is 5.6 m/s for all results presented here. The Reynolds number based on the diameter of a circle of equivalent area (D = 3.54 mm) and bulk velocity is 1200.

The flow visualization light source is provided by a frequency doubled (532 nm), pulsed Nd:YAG laser operating at 10 Hz. The laser power is approximately 20 mJ per 12 nanosecond pulse. A combination of cylindrical and spherical lenses is used to produce either a vertical or horizontal laser sheet approximately 1 mm thick. The green light scatters off micron sized canola oil droplets which have been seeded into the methane gas. Flow visualization images are recorded using a COHU model 6315 black and white CCD camera with a 50 mm lens. During the horizontal sheet measurements, the camera was positioned at a slight angle away from the axis of the jet to ensure that the flow did not impinge on the lens. Sequences of images are obtained by forcing the flow at 541 Hz. This results in a small phase difference between subsequent images, which are from different cycles. The video images are digitized and the contrast enhanced using OPTIMAS software. Figures 1 and 3 were taken with a 35 mm Nikon camera using Kodak Gold 400 speed film.

RESULTS

Figure 3a shows the region near the base of a split flame. The fuel jet was seeded and illuminated with a vertical sheet of light along the minor axis. Two toroidal roller structures are seen, along with a side jet to the left at 1.8 D. The plane of the ring inclines to the right. While this may suggest development of a helical instability, no evidence of a coherent helical structure is seen in horizontal images, presented below. Instead, inclination of the primary jet is likely due to conservation of momentum. Nevertheless, Chao, Jong and Tseng (1997) have shown that helical modes are capable of producing split ('branched') jets and flames. Figure 3b shows the structure in the reacting fuel jet at a lower forcing amplitude. The flame is unsplit ('classic' flame shape), no side jet formation is observed, and the rollers remain coaxial with the nozzle.

Figure 4 compares forcing conditions for splitting of the flame and of the nonreacting jet, in the region around 541 Hz. Forcing amplitudes measured by hot-wire in the non-reacting methane jet are also shown. Very low levels of forcing (<25%) are needed to cause the nonreacting jet to split, while significantly higher levels (~50%) are required before the flame responds. Thus, there is a range of conditions where the flame suppresses formation of side jets. For high levels of forcing at between 500 and 540 Hz, both the flame and the nonreacting jet are turbulent. At very high levels the flame cannot be stabilized. At frequencies above 550 Hz the flame exhibits bifurcation behavior at moderate forcing levels. In this regime the flame is intermittently split and transition from the classic diffusion flame to the split flame is spontaneous and rapid. As the frequency is increased, increasingly higher levels of forcing are required to maintain a constantly split condition. No state bifurcation was observed in the nonreacting jet.

Horizontal cross sections of the nonreacting jet reveal the topography of the split jet. Figures 5 and 6 are oriented with the minor axis pointing left to right. Phase angle is defined in each image plane relative to when the center of the roller passes through the plane. Figure 5a shows the jet at 0.9 D downstream of the nozzle exit when the phase angle is ϕ = 36 degrees. The center of the primary toroidal structure has just passed through the plane defined by the light sheet. Self induction has distorted the roller so that the portions along the minor axis are the last to pass through the image plane. Note that the formation of side jets along the major axis has begun less than one diameter downstream of the nozzle exit in the nonreacting jet. Splitting along the major axis is observed at 5.4 D in the nonreacting jet, although the flame splits along the minor axis beginning between 1.5 and 2 D downstream. Whether the flame suppresses splitting in the minor axis is not yet clear. The elliptic jet geometry was successful at stabilizing the azimuthal position of the side jet. Experiments with an annular flow of air around the nozzle have shown that a co-flow velocity of 3 to 4% of the jet velocity can also stabilize the position of the side jets, while a co-flow of more than 5% suppresses the formation of side jets. There is evidence of pairs of streamwise vortex structures just outside of the

roller, with the structures at one end of the major axis slightly more developed than those at the other.

Figure 5b is at ϕ = 180°, when the 'braid' region, defined as the region between the rollers, is passing through the image plane. Two pairs of streamwise vortex structures are now clearly visible near the jet centerline, otherwise, there is very little other fluid left in the core of the jet. Some fluid is seen outside the jet, attached to one end of the major axis. This fluid was probably ejected in a previous cycle, and represents the upstream extent of a side jet.

Figures 6a-c show one cycle of the forcing at 1.8 D downstream. Two side jets, oriented along the major axis, have formed, ejecting fluid over 3.25 D from the central jet. Figure 6a, at ϕ = 0°, shows that the roller has switched axes due to self induction (Ho and Gutmark, 1987), and the major axis is now perpendicular to the orientation of the nozzle's major axis. Pairs of streamwise vortex structures are clearly seen in the side jets adjacent to the roller. Additional structure is seen in the side jets further from the roller, suggesting that fluid there was ejected in streamwise structures in previous cycles. In Fig. 6b, taken in the braid region, no jet fluid remains on the centerline, and no clear streamwise structures are seen near the core of the jet, although some are visible further away from the jet axis. Streamwise structures reappear near the jet core in Fig. 6c, taken as the top of the roller enters the image plane.

Explanations for the formation of side jets (Monkewitz and Pfizenmaier, 1991; Brancher et al., 1994) in nonreacting flow focus on an interaction between rollers and streamwise braid structures which causes jet fluid to be ejected from between braid pairs. However, this model of vortex structure does not differ significantly from accepted descriptions of shear layers that do not exhibit the perpendicular ejection of fluid. We propose that side jets are the result of a reconnection event involving pairs of streamwise braid structures. The resulting loops then propagate perpendicular to the jet due to self induction, as suggested in Figure 7. Self induction thus provides the mechanism for convection of fluid far from the jet. This hypothesis is supported by the evidence of streamwise vortex structures in the side jets, and the position of braid structures relative to the rollers as described above. Also, an additional vortex structure of the same sign as the roller is consistently observed near the top of the roller (Carlton et al. 1998), near the lower edge of the side jet and may represent the bottom of the braid loop. Whether the top of the braid loop detaches from the roller is not clear from our data. Lasheras and Prestridge (1997) also propose that self induction is responsible for side jets: their mechanism involves pinching of the roller to create vortex loops. However, they report a gradual amplification of the azimuthal instability that leads to side jet formation. No evidence of pinching is seen on our primary vortex ring, and the side jet forms at a specific downstream location. Thus we speculate that different physical phenomena have been observed.

CONCLUSIONS

An elliptic, nonreacting methane jet was observed to split along both the major and minor axes under strong axial velocity perturbation. Flow visualization shows the presence of side jets, oriented along the major axis of the nozzle, as early as 0.9 D downstream of the nozzle exit. These side jets develop as the primary rollers move downstream. The horizontal cross-section images reveal evidence of streamwise vortex structures present in the side jets. Based on these results, a new mechanism for the formation of side jets has been proposed which involves a reconnection of streamwise braid structures to form vortex loops that convect away from the central jet. Side jets in the fuel jet result in a split flame. However, the flame requires a higher level of excitation to split than does the nonreacting jet, and displays a state bifurcation between split and classic jet diffusion flame at moderate forcing in some frequency ranges. Flow visualization shows that the flame acts to suppress all side jets at low forcing levels.

The flame's ability to suppress side jet formation, and its bifurcation behavior raise interesting questions about the nature of the instability that causes side jets. For example, side jets have been observed in both highly forced and absolutely unstable jets; by what mechanism is the flame able to influence the global or local stability of the flow? Additional information regarding the influence of boundary conditions such as co-flow on split jets is also needed. Understanding this phenomenon may lead to much greater control over these flames. Future work will include two-dimensional velocity and vorticity measurements of the reacting and nonreacting jet as well as computational modeling of the system. Studies under a variety of gravity conditions are under way as well.

ACKNOWLEDGMENTS

This work is supported by the Microgravity Combustion Science Branch of NASA under Grant NAG3-1616. Our thanks also go to Brian Aiken for his help with the apparatus.

REFERENCES

Brancher, P., Chomaz, J.M., and Huerre, P., 1994, "Direct numerical simulations of round jets: Vortex induction and side jets", *Physics of Fluids*, 6 (5): 1768-1774.

Carlton, J., Hertzberg, J., Davis, E. and Linne, M., J., 1998, "Splitting of forced elliptic jets and flames", *Flow Visualization and Image Processing*, Vol. 5, pp. 155-165.

Chao, Y.-C., Jong, Y.-C. and Tseng, Z.-H., 1997, *Proceedings of the 1st Pacific Symposium on Flow Visualization and Image Processing*, pp. 513-518.

Clemens, N.T., and Paul, P.H., 1995, "Effects of heat release on the near field flow structure of hydrogen jet diffusion flames", *Combustion and Flame,* 102, pp. 271-284.

Hertzberg, J., 1997, "Conditions for a Split Diffusion Flame", *Combustion and Flame*, 109, pp. 314-322.

Ho, C.M., and Gutmark, E., J. 1987, Fluid Mech., 179:383-405.

Hosangadi, A., Merkle, C.L., and Turns, S.R., 1990, "Analysis of forced combustion jets", *AIAA Journal*, 28(8):1473-1480.

Katta, V.R., and Roquemore, W.M., 1993, "Role of inner and outer structures in transitional jet diffusion flame," *Combustion and Flame*, 92, pp.274-282.

Lasheras, J., and Prestridge, K., 1997, "AIAA 97-1880", *28th AIAA Fluid Dynamics Conference and 4th AIAA Shear Flow Control Conference*.

Mahalingam, S., Cantwell, B.J., Freezer, J.H., 1990, "Full numerical simulation of coflowing, axisymmetric jet diffusion flames", *Physics of Fluids* A 2(5), pp. 720-728.

Monkewitz, P.A., and Pfizenmaier, E., 1991, "Mixing by 'side jets' in strongly forced and self-excited jets", *Physics of Fluids* A, 3(5): 1356-1361.

Schemer, R. W., Namibian, M., Filtopoulos, E.E.J., Kelly, J., 1994, "Temporal evolution of turbulence/chemistry interactions in lifted turbulent jet flames," *25th Symp. (Int'l) on Combustion*, In press, Combustion Institute.

Figure 1: Split flame.

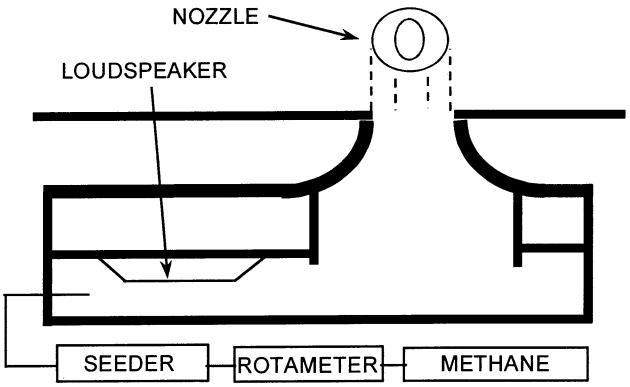

Figure 2: Experimental schematic.

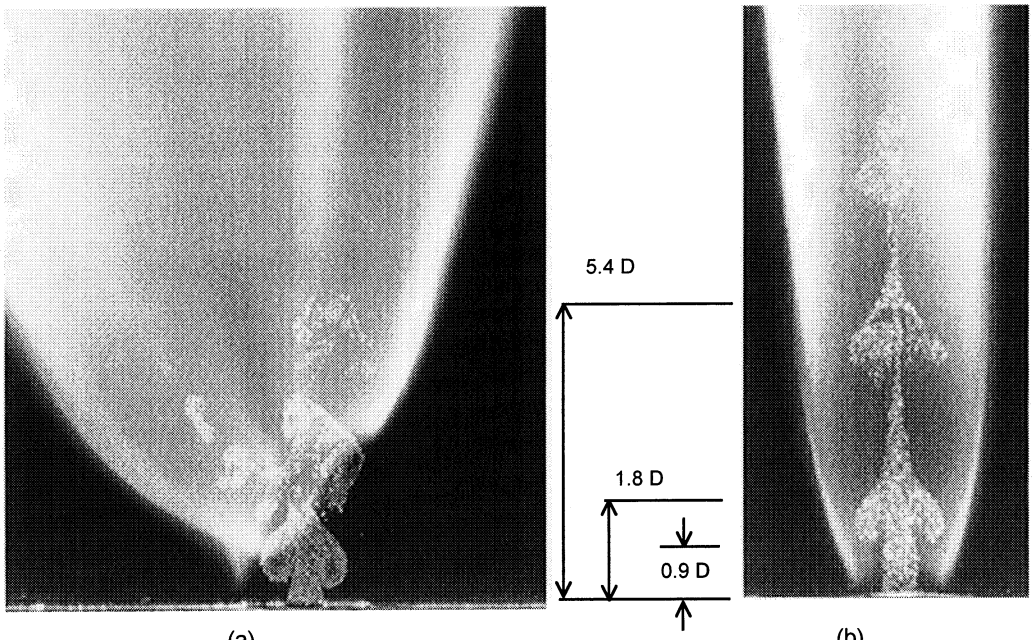

Figure 3: Reacting $\frac{210}{\text{jet}}$ jet (a) and unsplit jet (b).

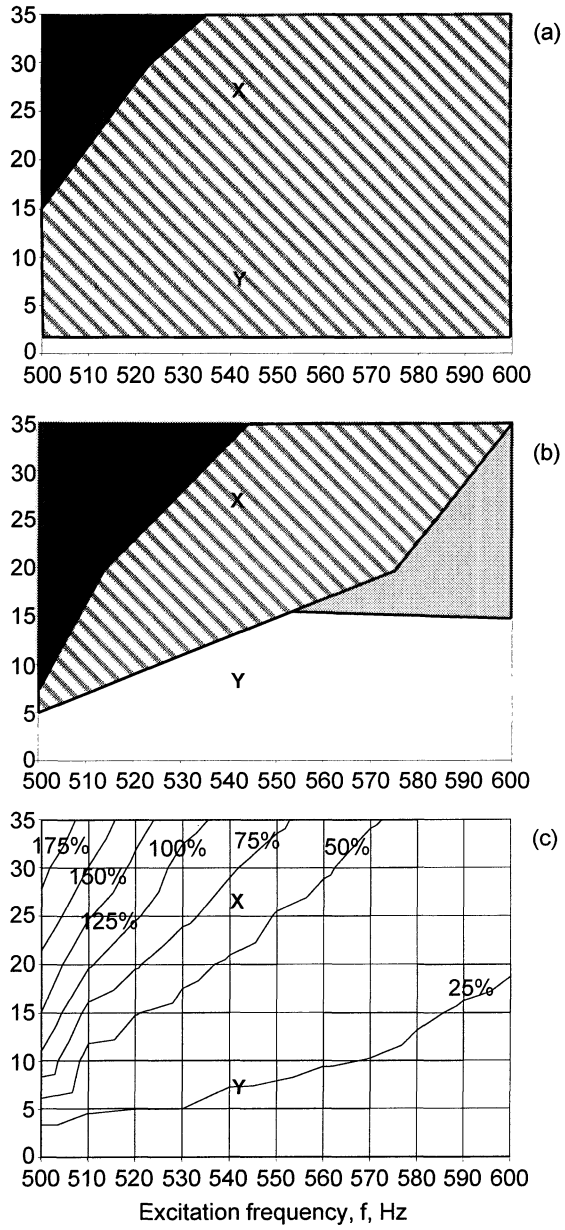

Figure 4: Acoustic response of reacting jet (a) and nonreacting jet (b) and velocity perturbation magnitude (c) as a percentage of bulk velocity (5.6 m/s).

Bifurcation: turbulent lifted/ split flame or turbulent jet

Bifurcation: split flame/ classic diffusion flame

Split flame or jet

Classic diffusion flame or non-reacting jet

X Conditions for split flame results presented here

Y Conditions for forced unsplit flame presented here

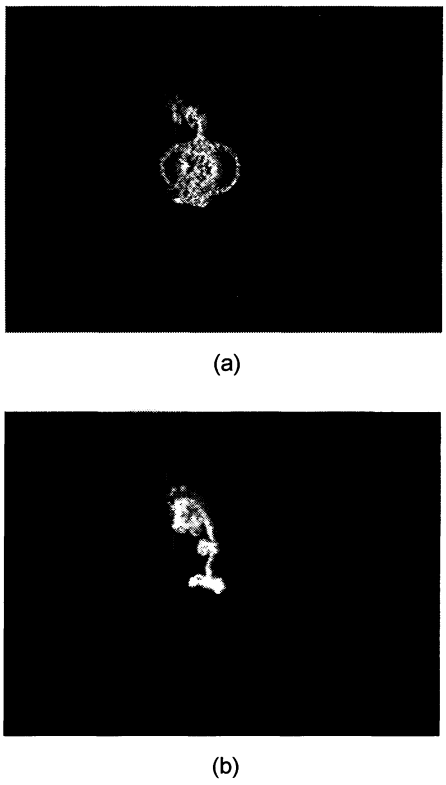

Figure 5: Horizontal cross section of a nonreacting, normal gravity, split jet at 0.9 D downstream. Phase difference of 180 degrees between (a) and (b).

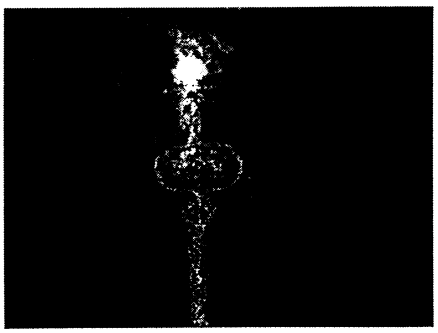

(a) Phase angle = 0

(b) Phase angle = 108

(c) Phase angle = 252

Figure 6: Horizontal cross section of nonreacting, normal gravity, split jet at 1.8 D downstream.

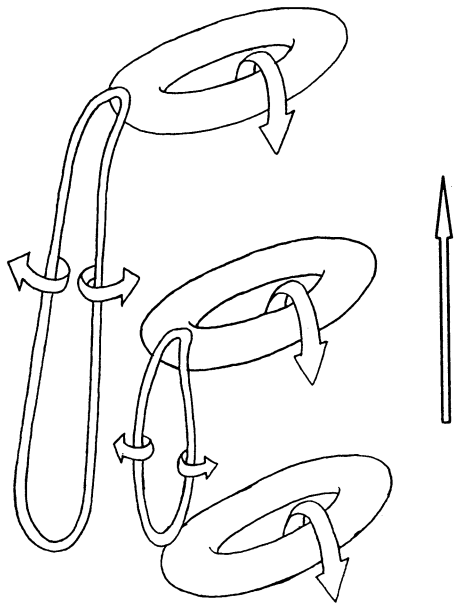

Figure 7: Proposed side jet formation mechanism. Arrow denotes direction of bulk velocity.